

Specific wetting probed with biomimetic emulsion droplets

Jacques Fattaccioli,^{*a} Jean Baudry,^a Nelly Henry,^b Francoise Brochard-Wyart^b and Jérôme Bibette^a

Received 21st April 2008, Accepted 28th July 2008

First published as an Advance Article on the web 3rd October 2008

DOI: 10.1039/b806635c

We have produced emulsion droplets of controlled size and composition coated by ligands, and studied the adhesion of these drops on a solid substrate coated by receptors and polymers. Using transmission, RCM and fluorescence microscopy we assess the size, contact angle and ligand density for each drop. We first show that non-specific interactions significantly enhance the proteins density within the adhesive patch. Then we show that binding within the patch is partially inhibited in good agreement with the hypothesis of an absence of translational diffusion. We confirm that the density of specific bonds sets the adhesive energy and therefore the final contact angle, and finally show that specific binding in our system is always associated with the existence of a positive line tension, which linearly increases with the density of receptors. These experiments describe a new scenario for specific wetting which raises the importance of the coupling between non-specific interactions and specific binding.

Introduction

Emulsion droplets stabilized by a surfactant monolayer as well as lipid bilayer vesicles can wet both liquid or solid interfaces. The wetting-induced adhesion can be described by the Young–Dupré equation $\varepsilon = \gamma(1 - \cos\theta)$, where ε is the energy of adhesion, γ the surface tension, and θ the contact angle. Wetting can also arise from the specific association between surface bound ligands and receptors. From this perspective, the first theoretical description was proposed by Bell and coworkers¹ for the case where binders are free to diffuse. This model involves a specific affinity between dilute ligands and receptors that superimposes onto short-range membrane repulsion; the adhesive energy is then predicted to be proportional to the homogeneous binder surface concentration within the adhesive patch. Certainly because of their similarity with cell membranes, liposomes^{2–6} were the first systems to be used to check Bell's predictions. Following these pioneering works, more detailed behaviors have been reported highlighting the possible existence of a two-dimensional phase transition when non-specific repulsive forces compete with adhesive biomolecules^{7,8} or the effect of the size of the repellers on the adhesive pattern.⁹

In this work we employ emulsion droplets as a novel biomimetic model system and streptavidin–biotin as a model ligand–receptor pair. Using these biomimetic systems we reveal important consequences of the role of non-specific interactions on the structure of the interface of the adhesive liquid both at the colloidal and molecular scale. It is shown that these non-specific interactions can significantly enhance the ligand density into the adherent zone. Indeed, once proteins are grafted on the liquid surface their entropy is significantly reduced, which in turn facilitates the spontaneous formation of condensed states. This occurs as a result of any weak non-specific interactions between proteins and their surrounding medium within the confined

layer. Consequently, since in our case the substrate is solid and the proteins self-condense into a solid layer, the specific binding takes place in the absence of any translational diffusion. This causes a large decrease in the final density of specific bonds. However, we confirm that the density of specific bonds still sets the adhesive energy and therefore the final contact angle. Finally, we show that specific binding in our case is always associated with the existence of a positive line tension, which linearly increases with the density of receptors.

Experimental

Biotin and streptavidin

As a model ligand–receptor pair, we chose the biotin–streptavidin complex, which is extensively described in the literature, highly stable and easy to handle.^{10,11} Biotin, also known as vitamin H or B₇, is a water-soluble vitamin widely used in biochemical assays. Streptavidin is a 53 kDa tetrameric protein purified from the bacterium *Streptomyces avidinii*. It finds wide use in molecular biology through its extraordinarily strong affinity for biotin; the dissociation constant (K_d) of the biotin–streptavidin complex is of the order of $\sim 1 \times 10^{-15}$ mol L⁻¹, ranking among the strongest known non-covalent interactions.

Characterization by microscopy

All the microscopic observations are carried out with a Nikon Eclipse upright microscope and a 100× immersion oil objective linked to a Hamamatsu ORCA ER-1394 12-bit camera and controlled by the Mediacybernetics Image-Pro Plus image processing software. We use ND attenuation filters for the quantitative measurements of the fluorescence intensities in order to eliminate photobleaching in the timescale of our experiments.

Fabrication of the streptavidin functionalized emulsion

We disperse soybean oil (Sigma-Aldrich) at a fraction $\phi = 75\%$ w/w by gently stirring it in an aqueous phase comprising

^aLCMD, CNRS, UPMC, ESPCI - 10, rue Vauquelin, 75231 Paris Cedex 05, France

^bLaboratoire Physico-Chimie, Institut Curie, CNRS - 26, rue d'Ulm, 75005 Paris, France

15% w/w Poloxamer 188 block-polymeric surfactants [HO(C₂H₄O)₇₉(C₃H₆O)₂₈(C₂H₄O)₇₉H, Uniqema] and 2% w/w sodium alginate (Sigma-Aldrich) used as a thickening agent. In order to get monodisperse droplets, we further shear this crude polydisperse emulsion in Couette cell apparatus under a controlled shear rate of 5000 s⁻¹, following the method developed by Mason and Bibette.¹² After fragmentation, the final diameter of the droplets is equal to 5 ± 1 μm. Within this size range, droplets can be observed with a microscope and characterized by a flow cytometer as explained below. For storage and handling purposes, we dilute the emulsion to an oil fraction of φ = 60% w/w with 1% w/w of Poloxamer 188 in the continuous phase and we store the aliquots at 11 °C for up to several weeks.

Functionalization of the emulsion droplets

Soybean oil contains some free acidic molecules,¹³ from the oleic acid family, which at neutral pH become surface active, making it possible to functionalize the carboxylic groups with compounds bearing an NH₂-moiety *via* the formation of a peptidic bond.¹⁰ We choose first to graft a biotin derivative, biotin-(C₂H₄O)₃-NH₂ (C₁₆H₃₀N₄SO₄, Interchim), and then to bind fluorescent streptavidin to the biotins (Fig. 1).

Biotin attachment. The first step relies on the attachment of a small amino-biotin derivative to the carboxylic groups, which is activated by a carbodiimide coupling agent and a stabilizer. (i) *Activation of the carboxylic groups:* we dilute 17 μL of emulsion in a Phosphate-Tween20 buffer (PB-Tween20) in a 500 μL microtube to obtain 200 μL of a suspension at φ = 5% w/w. The PB-Tween20 buffer has an ionic strength of 20 mM, a pH = 7.3 and contains 0.2% w/w (~3CMC) of Tween20 surfactant

[mono-9-octadecanoate poly(oxy-1,2-ethanediyl), Sigma-Aldrich]. The suspension is then gently mixed for 30 min with 50 μL of the activation solution containing 30 mg of EDAC (*N*-ethyl-*N'*-(3-dimethylaminopropyl)-carbodiimide hydrochloride, Sigma-Aldrich) and 5 mg of sNHS (Sulfo-*N*-Hydroxy-Succinimide, Sigma-Aldrich) in the PB-Tween20 buffer. At the end of this reaction, we wash the suspension by removing 230 μL of the continuous phase and adding 180 μL of PB-Tween20. (ii) *Amino-biotin linkage:* 50 μL of a solution of biotin-(C₂H₄O)₃-NH₂ (Interchim) in PB-Tween20 at a concentration C_{biot} is added to the activated suspension and the tube content is slowly mixed for 30 min. C_{biot} ranges between 0.5 and 6 mg mL⁻¹ in a PB-Tween20 buffer. At the end of the reaction, we wash the suspension 8 times with the PB-Tween20 buffer in order to remove the free amino-biotin molecules from the solution.

Streptavidin adsorption. We complex either AlexaFluor® 555-conjugated streptavidin (Molecular Probes-Invitrogen) or fluorescein isothiocyanate (FITC)-conjugated streptavidin (Interchim) onto the biotin molecules. Since we introduce streptavidin in excess as compared to the available biotins on the surface, the density of biotins sets the streptavidin density on droplets, $\Gamma_{\text{droplet}}^s$, at the end of the reaction. For flow cytometry characterization, to fit with the laser wavelength of the instrument, we use FITC streptavidin. In a 500 μL microtube, we rinse 10 μL of the biotinylated emulsion with a MES-Tween20 buffer. This buffer has a MES concentration [2-(*N*-morpholino)ethanesulfonic acid, Sigma-Aldrich] of 20 mM, pH = 5.3 and a Tween20 concentration of 0.2% w/w. Then, we mix the suspension for 15 min with 5 μL of the streptavidin solution (C_{strep} = 0.1 mg mL⁻¹ in a MES-Tween20 buffer) and 25 μL of MES-Tween20 buffer. At the end of the adsorption process and before the adhesion experiments, we rinse the suspension at least five times with a PB-Tween20 buffer to remove the free streptavidin within the bulk phase.

Characterization of the droplets by flow cytometry

The size of the droplets and their surface tension ($\gamma = 2 \text{ mN m}^{-1}$) are compatible with the use of a flow cytometer¹⁴ (Becton-Dickinson FACSCalibur). We previously demonstrated¹⁵ that it is possible to analyze the scattered light and to derive the radius R of the droplets individually. Moreover, thanks to a fluorescence calibration kit (Quantum FITC MESF High Level, Bangs Laboratories), it is possible to convert the mean fluorescence of each droplet into the number of fluorescent streptavidins, N_s , adsorbed on the surface. From these two independent measurements we can plot the density of expressed streptavidin as a number of proteins per square micron:

$$\Gamma_{\text{droplet}}^s(R) = \frac{N_s}{4\pi R^2} [\mu\text{m}^{-2}]$$

Since the streptavidin density $\Gamma_{\text{droplet}}^s(R)$ remains constant over the whole size distribution, it is then possible to estimate a mean streptavidin density that has been changed from $\Gamma_{\text{droplet}}^s = 65$ to 330 μm⁻². Streptavidin has a molecular surface area¹⁶ close to 30 nm², therefore the streptavidin densities used here correspond to roughly 1% of a theoretical full monolayer coverage.

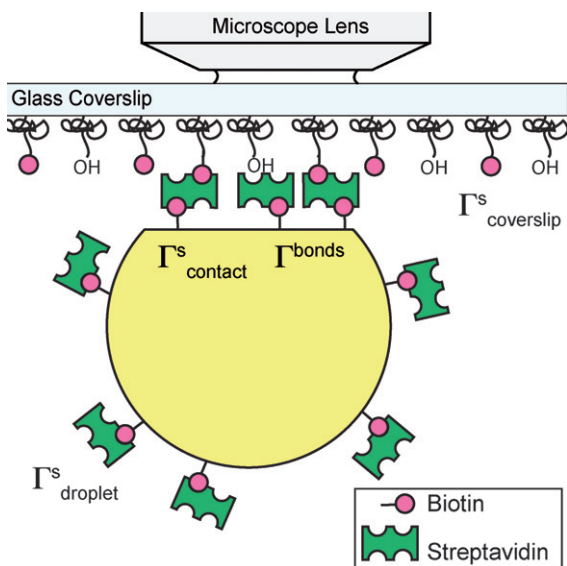


Fig. 1 A schematic representation of an emulsion droplet functionalized by mobile fluorescent streptavidins ($\Gamma_{\text{droplet}}^s$) adhering to a solid glass coverslip covered by PEG-biotin polymers ($\Gamma_{\text{coverslip}}^s$). Streptavidins are captured in the contact area ($\Gamma_{\text{contact}}^s$) but a fraction of them are bound to PEG-biotin (Γ_{bonds}^s). The observation is carried out with an upright microscope allowing us to measure the fluorescence intensity of the contact zone, its radius, and the radius of the droplet.

Fabrication of the biotinylated solid substrates

The solid biomimetic substrates (Fig. 1) are made from glass coverslips (Erie Scientific) coated first by poly-L-lysine (PLL, Sigma-Aldrich) and then grafted with a brush of mixed poly(ethylene)glycol macromolecules such that a fraction of them are terminated by biotin.^{17,18} The solution we use for the functionalization is an NHS-(C₂H₄O)₄₆-OH (NHS-PEG-OH, MW = 2000 g mol⁻¹) and NHS-(C₂H₄O)₇₈-biotin (NHS-PEG-biotin, MW = 3400 g mol⁻¹) mixture. The total bulk concentration of polymeric chains C_{PEG} + PEG_{biot} is kept constant at 200 μM, although the ratio

$$R_{\text{PEG}} = \frac{\text{NHS-PEG-biotin}}{\text{NHS-PEG-biotin} + \text{NHS-PEG-OH}}$$

varies from 0 to 100%. We dilute the NHS-PEG-OH and NHS-PEG-biotin powders purchased from Nektar Therapeutics with DMF (*N,N*-dimethylmethanamide, Sigma-Aldrich) at a concentration of 50 mM. We split the solutions into aliquots and store them at -20 °C in order to avoid hydrolysis of the NHS-moiety.

Prior to the grafting process, we clean the glass coverslips in a hot Piranha mixture (H₂SO₄-H₂O₂, 15 min) and we rinse them thoroughly in DI water for several minutes. Then the coverslips, distributed individually in multiwell plastic plates used for cell culture (Fisher Scientific), are rinsed two times with 2 mL of PBS (Gibco-Invitrogen) each. The use of multiwell plates helps in achieving good reproducibility of the functionalization for all coverslips from the same cleaning batch. Then, we add 2 mL of 0.01% w/w PLL solution in PBS to each well and we store the coverslips overnight in a humid incubator at 37 °C. After four rinsing steps with 2 mL of PBS, we pour 1 mL of the functionalization solution into each well and we incubate the coverslips at 37 °C for 30 min to complete the reaction. Finally, we very carefully rinse the wells 8 times with 2 mL of PBS and we store the plates at 4 °C before running the adhesion experiment within the same day.

Characterization of the biotinylated substrates

In our adhesion experiments, the relevant characteristics of the functionalized glass substrates are less their PEG-biotin density than the maximal density of streptavidin $\Gamma_{\text{coverslip}}^{\text{s}}$ that they are able to bind. This *binding capacity* is determined indirectly¹⁷ by first dipping the coverslips in a solution of Alexa Fluor® 555 streptavidin in excess compared to the available biotin molecules on the surface (0.05 mg mL⁻¹ in PBS with 0.2% w/w Tween20), and then by performing an absolute bulk measurement of the concentration (C_{∞}) of unbound streptavidin in the supernatant at the chemical equilibrium (15 min at room temperature). Since we measured the initial streptavidin concentration (C_0) prior to the chemical reaction, the streptavidin density on the glass coverslips is:

$$\Gamma_{\text{coverslip}}^{\text{s}} = \frac{(C_0 - C_{\infty}) \times (\text{supernatant volume})}{\text{surface of the coverslip}}$$

In Fig. 2 (top), we plot the streptavidin density on the glass coverslip as a function of the NHS-PEG-biotin ratio R_{PEG} expressed as a percentage. The streptavidin density $\Gamma_{\text{coverslip}}^{\text{s}}$

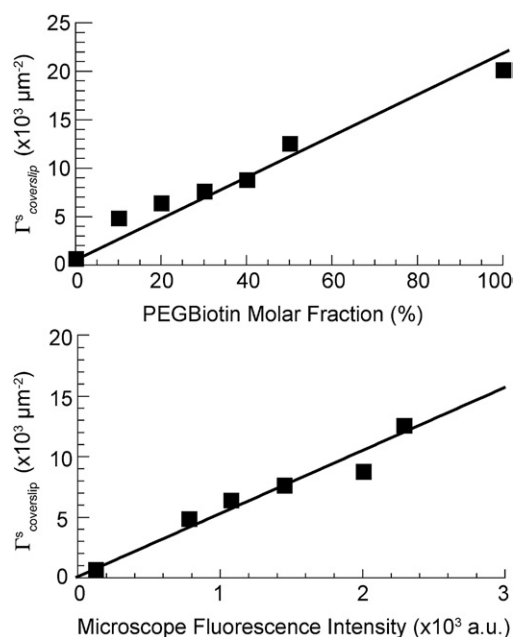


Fig. 2 (top) The density of the streptavidin $\Gamma_{\text{coverslip}}^{\text{s}}$ as a function of the NHS-PEG-biotin ratio R_{PEG} ranging from 0 to 100%, corresponding to the measurement of the fluorescence done by spectrofluorometry. The linear dependence indicates that no steric hindrance is involved in the adsorption process. (bottom) We calibrate the intensity of fluorescence measured by the microscope with the corresponding bulk measurement of fluorescence performed with the spectrofluorometer.

increases linearly with the density of PEG-biotin on the glass coverslips, showing that there is no hindrance of the adsorption process in this range of streptavidin and PEG-biotin concentrations.

In the experiments reported in this article, we aim to measure the absolute density of streptavidin captured in the contact zone of the droplet with the glass substrate. Therefore, we used the bulk measurement of the unbound streptavidin concentration in the supernatant to calibrate the measurement of the fluorescence intensity of the coverslips measured with an epifluorescence microscope and a CCD camera. This is achieved by rinsing 4 times with 2 mL of PBS, mounting on a glass slide under the microscope measuring their intensities. In Fig. 2 (bottom), we plot the density of streptavidin $\Gamma_{\text{coverslip}}^{\text{s}}$ on the glass surface as a function of the intensity of fluorescence and we show that the binding capacity of the solid substrates increases linearly with the epifluorescence intensity over the whole range of PEG-biotin ratios.

Results and discussion

We inject a buffered suspension containing a few hundred emulsion droplets covered with streptavidin at a density, $\Gamma_{\text{droplet}}^{\text{s}}$, in a 50 μm thick chamber made of a functionalized glass coverslip on the top, a microscope glass slide on the bottom and double-sided tape as a spacer. To avoid evaporation we handle the glass containers in a humid chamber made from a Petri dish and some wet wiping paper. Driven by a pN buoyancy force each droplet hits the top slide, which has been functionalized with a density $\Gamma_{\text{coverslip}}^{\text{s}}$ of PEG-biotin, within a few seconds and stays in

contact with the slide over several tens of minutes (Fig. 1). The adhesion is irreversible and occurs in less than five minutes.

For each droplet we record the radius, R , from direct transmission microscopy, the adhesion zone radius, ρ , from reflection interference contrast microscopy¹⁹ (RICM), and finally the spatial distribution of fluorescent streptavidin within the adhesion zone from an epifluorescence intensity measurement. Fig. 3 shows images of droplets coated with $\Gamma_{\text{droplet}}^{\text{s}} = 330$ streptavidins per μm^2 , and adhering on two different types of glass substrates: the first one (a) being only functionalized by PEG–OH ($\Gamma_{\text{coverslip}}^{\text{s}} = 0 \mu\text{m}^{-2}$) while the other (b) is fully covered by PEG–biotin ($13 \times 10^3 \mu\text{m}^{-2}$). The epifluorescence images show the overlay of an equatorial view of the droplets (*red*) and a view of the adhesion zones on the coverslip (*green*). Before discussing the details of the results, we notice that in both cases fluorescent adhesion zones are visible. The intensity of the *green* layer is higher than the intensity of the *red* layer, so we use two different gain parameters for the two layers within the same picture.

There are two possible causes for the increase in the fluorescence intensity: an accumulation of proteins into the contact zone or an enhancement of the fluorophore quantum yield due to confinement and the surrounding environment. However, when droplets adhere to the coverglass, we always find that the overall fluorescence intensity of the unbound region of the droplets decreases, while we observe a corresponding increase in the fluorescence intensity of the bound region. When this region becomes large enough, we even observe a complete loss of fluorescence intensity from the spherical, unbound region of the

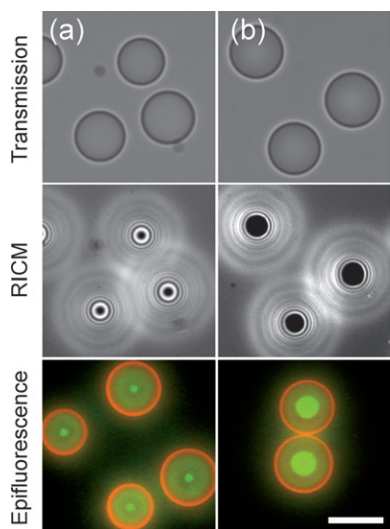


Fig. 3 Transmission, RICM and epifluorescence micrographs of emulsion droplets coated with $\Gamma_{\text{droplet}}^{\text{s}} = 330 \mu\text{m}^{-2}$, adhering to biotin-functionalized glass coverslips. We obtain the fluorescent images by overlaying a view of the adhesion zones (*green*) and a corresponding equatorial view of the droplets (*red*) with different gain parameters. (a) No biotin molecules are present on the coverslip, but the droplets adhere, as shown by the existence of a black contact zone on the RICM picture and an enrichment of streptavidin density; (b) the substrate has the same overall PEG surface density but here $\Gamma_{\text{coverslip}}^{\text{s}} = 13 \times 10^3 \mu\text{m}^{-2}$. In this case, the contact surface increases as compared to the preceding case (scale bar = 5 μm) and the enrichment of streptavidin density persists within the patch.

droplets. This suggests that all of the streptavidin is driven toward the adhesion zone. By dividing the total number of streptavidin molecules adsorbed onto the droplets by the surface area of the adhesion zone, we find good agreement of the density of streptavidins in the contact region with what we measure by fluorescence microscopy (see Experimental section). Moreover, by decreasing the ratio of fluorescent to non-fluorescent streptavidin molecules covering the emulsion droplets, we observe a corresponding decrease in fluorescence intensity in the contact zone by the same ratio, either with AlexaFluor® or FITC streptavidin. This observation rules out interactions between adjacent fluorophores. Finally, if we manually apply some pressure on the microchamber, the flow of liquid pulls some droplets from the functionalized coverslip and reveals small patches of fluorescent streptavidins still bound to the glass. The fluorescence intensity of these patches has nearly the same value as the fluorescence intensity of the contact zone of droplets remaining attached to the coverglass. The oil droplet has no influence on the fluorescence intensity of the streptavidins captured within the adhered region.

On the basis of these conclusions we can thus quantitatively analyze our microscope pictures. We can indeed see that in Fig. 3(a), which corresponds to the absence of PEG–biotin, $\Gamma_{\text{coverslip}}^{\text{s}} = 0$, a relatively small and flattened adhesive patch is still visible on both pictures obtained either from epifluorescence or RICM. This must arise from droplet–substrate non-specific interactions since specific receptors are absent. Moreover, this weak wetting is still present in the absence of streptavidins and we noticed that it is very sensitive to both the nature of the adsorbed surfactant stabilizer and pH but not to the ionic strength of the buffer. Moreover, since the patch remains more fluorescent than the rest of the droplet surface, we must conclude that ligands are driven within the patch by some affinity that they experience within the confined film. PEG polymers are generally known and used to avoid protein adsorption. However, in our case this accumulation only occurs within the confined adhesive zone and is not observed on our solid substrate with streptavidins in solution (see Experimental section). Moreover, previous results have already reported some evidence for a detectable affinity between streptavidins and poly(ethyleneglycol)²⁰ in confined geometries. We believe this effect originates from the reduction of entropy when proteins are grafted which in turn facilitates the persistence of condensed states.²¹ In Fig. 3(b) the presence of biotins on the substrate clearly leads to a larger adhering patch, which is again associated with an accumulation of ligands. This is so far in qualitative agreement with the predictions of Bell *et al.*¹ and with previous experiments on vesicles.

In order to quantify the recruitment of streptavidin in the contact area we repeat the same experiment as in the previous paragraph with five substrates having an increasing PEG–biotin density $\Gamma_{\text{coverslip}}^{\text{s}}$. We deduce the density of fluorescent streptavidin within the adhesion zone $\Gamma_{\text{contact}}^{\text{s}}$ from the measurement of the absolute fluorescence intensity (see Experimental section). In Fig. 4, we show the results obtained by averaging the fluorescence intensities over 50 droplets for increasing PEG–biotin densities $\Gamma_{\text{coverslip}}^{\text{s}}$. The streptavidin density $\Gamma_{\text{contact}}^{\text{s}}$ within the contact area is constant and does not depend whatsoever on $\Gamma_{\text{coverslip}}^{\text{s}}$, although it depends slightly on the mean droplet

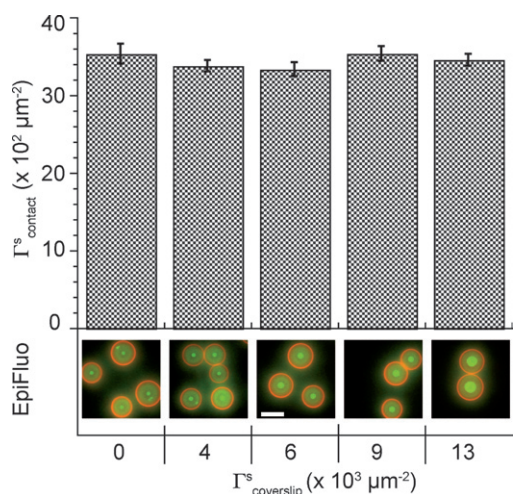


Fig. 4 We plot the streptavidin density in the contact area $\Gamma_{\text{contact}}^s$ as a function of the *binding capacity* $\Gamma_{\text{coverslip}}^s$ of the substrate for emulsion droplets coated with a density of streptavidin $\Gamma_{\text{droplet}}^s = 330 \mu\text{m}^{-2}$. We also show the corresponding dual-color epifluorescence pictures (scale bar = 5 μm) of the contact zone (*green*) and the equatorial region (*red*) of the adhering droplets. Whereas the size of the contact area increases with the density of biotin $\Gamma_{\text{coverslip}}^s$, the streptavidin density in the adhesion zone $\Gamma_{\text{contact}}^s$ remains constant.

density of streptavidin $\Gamma_{\text{droplet}}^s$, as shown in Fig. 5. We also show in Fig. 4 the epifluorescence images, for droplets having the same size in order to compare. Whereas the streptavidin density $\Gamma_{\text{contact}}^s$ in the adhesion zone is constant, the size of this zone and hence the contact angle depends linearly on binding capacity $\Gamma_{\text{coverslip}}^s$, as shown in Fig. 6. We can thus conclude that the streptavidin density $\Gamma_{\text{contact}}^s$ is not dictated by specific recognition whereas the size of the patch is.

To clarify this apparent contradiction, we propose to determine the density of specific bonds, Γ^{bonds} , that form within the adhesive patch, as a function of $\Gamma_{\text{coverslip}}^s$. To do so, we precisely measure the adhesive energy in order to deduce the density of biotin–streptavidin pairs that participate in the wetting process. When a droplet adheres, the energy of adhesion ε is related to the contact angle through the Young–Dupr e equation given by $\varepsilon = \gamma(1 - \cos\theta)$, where θ is the external macroscopic contact angle that can be expressed as:

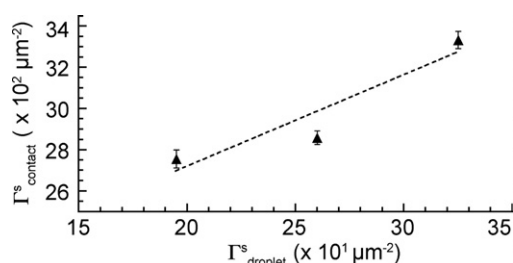


Fig. 5 The density of streptavidin $\Gamma_{\text{contact}}^s$ in the contact area, with $\Gamma_{\text{coverslip}}^s = 13 \times 10^3 \mu\text{m}^{-2}$, plotted with respect to the mean density of streptavidin on the droplets $\Gamma_{\text{droplet}}^s = 200, 260$ and $330 \mu\text{m}^{-2}$. The density $\Gamma_{\text{contact}}^s$ depends slightly on the overall density $\Gamma_{\text{droplet}}^s$ of streptavidin on the droplets.

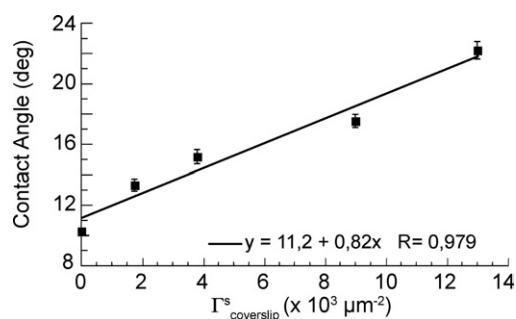


Fig. 6 The evolution of the macroscopic contact angle of adhering droplets with respect to $\Gamma_{\text{coverslip}}^s$ for emulsion droplets coated with a density of streptavidin $\Gamma_{\text{droplet}}^s = 260 \mu\text{m}^{-2}$. The contact angle increases linearly over the whole range of substrate densities and the non-specific contact angle is about 10° .

$$\begin{cases} \sin\theta = \frac{\rho}{R} \\ \cos\theta = \cos\theta_0 + \frac{\tau}{\gamma\rho} \end{cases} \quad (1)$$

if we consider in addition a line tension²² τ . We take advantage of the slight emulsion polydispersity to make a statistical measurement and plot the radius of the contact area ρ as a function of the droplet radius R from recording the entire population adhering on the cover slip. In Fig. 7 (top) we show a typical set of data $\rho(R)$ obtained from two substrates, one (\circ) having $\Gamma_{\text{coverslip}}^s = 0$, and the other (\square) having $\Gamma_{\text{coverslip}}^s = 13 \times 10^3 \mu\text{m}^{-2}$. In the presence of biotin on the substrate, the patch radius ρ is still linear with droplet radius, but the intercept is no longer zero. The existence of a line tension can explain this deviation, as shown in Fig. 7 (bottom). From the plot $\cos\theta(1/\rho)$ we can extract the slope τ/γ and the intercept $\cos\theta_0$ from a linear fit suggested by eqn 1. We note that a positive line tension

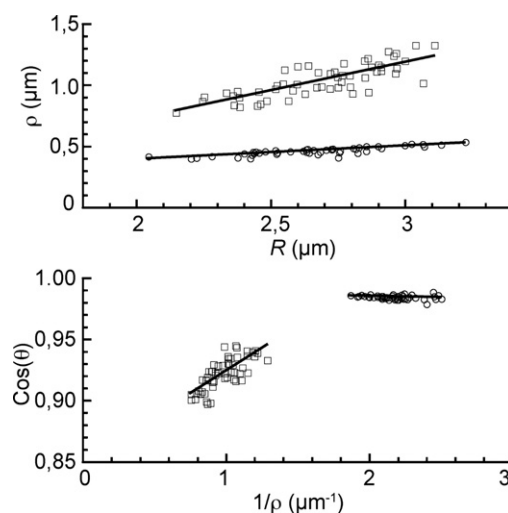


Fig. 7 We plot $\rho(R)$ (top) and $\cos\theta$ as a function of $1/\rho$ (bottom) for a typical set of data obtained from droplets coated with $\Gamma_{\text{droplet}}^s = 260 \mu\text{m}^{-2}$ that were adhering on two different substrates. The first had $\Gamma_{\text{coverslip}}^s = 0 \mu\text{m}^{-2}$ (\circ), and the other had $\Gamma_{\text{coverslip}}^s = 13 \times 10^3 \mu\text{m}^{-2}$ (\square). A positive line tension is always found in the presence of specific bonds and the adhesive energy is increased compared to the background.

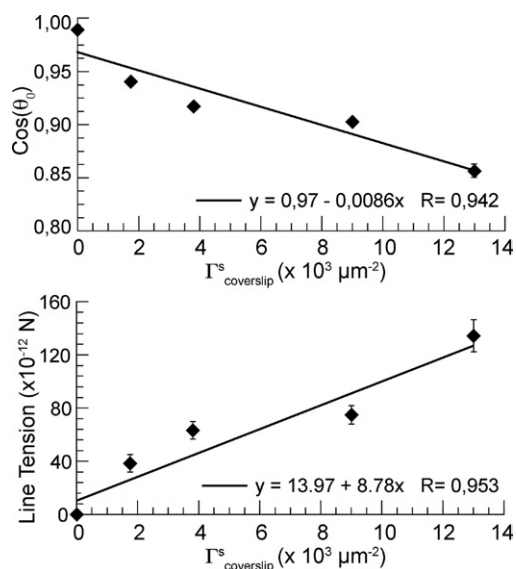


Fig. 8 We plot $\cos\theta_0$ (top) and τ (bottom) as a function of $\Gamma_{\text{coverslip}}^s$ obtained from droplets coated with $\Gamma_{\text{droplet}}^s = 260 \mu\text{m}^{-2}$. In the top graph the error bars are smaller than or as large as the markers that we use in this representation. The line tension ranges between 1×10^{-12} and 1×10^{-10} N and increases linearly on the whole range of PEG–biotin densities.

associated with a dewetting effect is systematically found in the presence of specific bonds and, as expected, the adhesive energy is increased when compared to the background. In Fig. 8, we plot $\cos\theta_0$ (top) and τ (bottom) as a function of $\Gamma_{\text{coverslip}}^s$. The line tension τ varies between 1×10^{-12} and 1×10^{-10} N and increases linearly with $\Gamma_{\text{coverslip}}^s$. These values are in agreement with the magnitude of the values reported in the literature.²² Although some theoretical papers have already reported that ligand–receptor couples could induce a line tension,^{23,24} the origin of such tension still remains unclear.

Since the surface energy of adhesion can originate from specific recognition as well as from inherent non-specific contributions, we formally rewrite the Young–Dupré equation as:

$$\varepsilon = \varepsilon_S + \varepsilon_{NS} - \varepsilon_{NS} = \gamma(\cos\theta_0^{NS} - \cos\theta_0^{S+NS}) \quad (2)$$

where ε is the adhesive energy due to specific bonds only within the contact zone, and where (S + NS) and (NS) refer to conditions such that specific bonds are eliminated, everything else being the same. In our regime of densely packed streptavidins, ε is simply the bond density times the energy per bond.^{1,24} From the difference given by eqn 2, we access the net specific contribution and by dividing this value by the energy per bond, we obtain the density of biotin–streptavidin couples Γ^{bonds} in the adhesion zone as a function of $\Gamma_{\text{coverslip}}^s$. We choose to approximate the value of the free energy per bond to the one obtained from the 3-dimensional affinity constant, measured elsewhere.¹¹ For $\Gamma_{\text{droplet}}^s = 330 \mu\text{m}^{-2}$ we observe a linear dependence (—) though the values of Γ^{bonds} are always smaller than the density of streptavidin in the contact zone $\Gamma_{\text{contact}}^s$ as plotted in Fig. 9. Thus we conclude that an important fraction of the streptavidins within the patch remains unbound although there is a large excess of biotins. To account for this we hypothesize that the

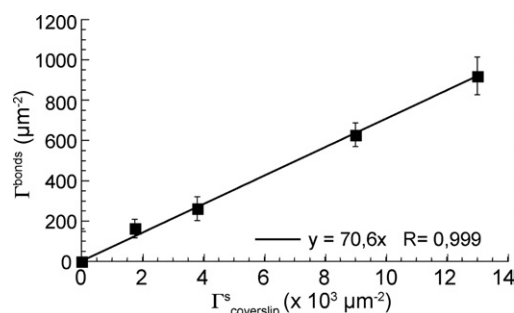


Fig. 9 The bond density within the patch Γ^{bonds} is plotted as a function of $\Gamma_{\text{coverslip}}^s$ for droplets coated with $\Gamma_{\text{droplet}}^s = 330 \mu\text{m}^{-2}$. The bond density shows a linear dependence (—). Its value is always lower than the streptavidin density $\Gamma_{\text{contact}}^s = 3300 \mu\text{m}^{-2}$.

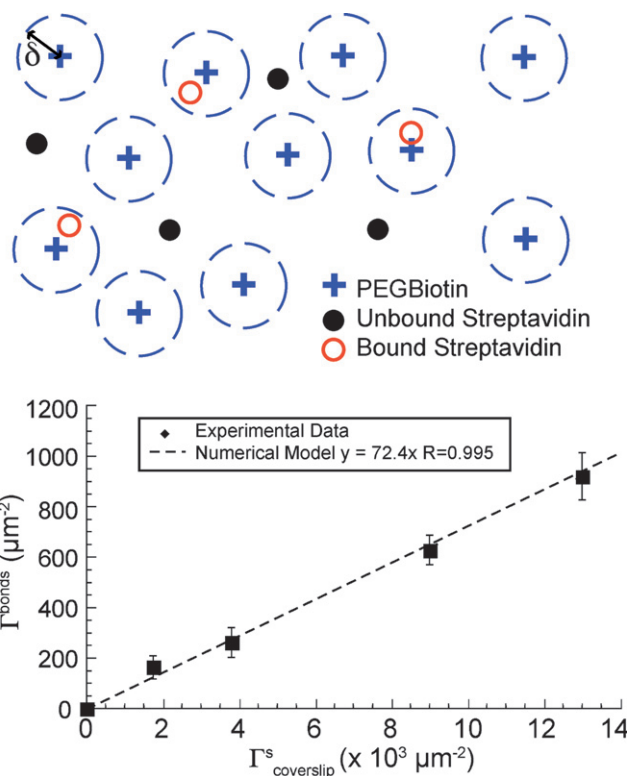


Fig. 10 (top) The simulation involves the superposition of two quasi-random lattices: one corresponding to the PEG–biotin on the surface (blue cross) and the other corresponding to the streptavidins trapped in the adhesion zone, which can be unbound from a biotin (black dot) or bound (red circle) if they fall within a distance smaller than δ from the closest biotin. The parameter δ is the only adjustable parameter of the model. (bottom) The bond density in the contact zone Γ^{bonds} is plotted as a function of $\Gamma_{\text{coverslip}}^s$ for droplets coated with $\Gamma_{\text{droplet}}^s = 330 \mu\text{m}^{-2}$. The experimental data are fitted numerically by computing the probability of two 2-dimensional quasi-random lattices having their nodes on the top of each other within an excursion distance δ with the lattices parameters deduced from $\Gamma_{\text{coverslip}}^s$ and $\Gamma_{\text{contact}}^s$. With an excursion length δ of the order of 2 nm, the numerical fit (----) shows excellent agreement with our data.

streptavidin translational diffusion is essentially arrested leading to a very poor capture efficiency.¹⁸ Therefore, we suggest that the accumulation of streptavidins induces a transition from liquid to solid as already described in analogous experimental situations.²⁵ Therefore the remaining dynamic responsible for the specific binding is supposed to arise mainly from the biotin and their flexible spacers.²⁶ As compared to a pure streptavidin monolayer, the streptavidin density in the contact zone is 10 times smaller (Fig. 4), but here the PEG layer interacts strongly with the streptavidin. We test this idea by computing the probability for two 2-dimensional quasi-random solid lattices to have their respective nodes on top of each other within an excursion distance δ as sketched in Fig. 10 (top). We deduce the lattice parameters from the measurements of $T_{\text{coverslip}}^{\text{s}}$ and $T_{\text{contact}}^{\text{s}}$. The simulation is very sensitive to the value of the unique adjustable parameter δ . We find excellent agreement with our data, as shown by the numerical fit in Fig. 10 (bottom), which finally leads to an excursion length $\delta = 2$ nm. The radius of gyration of poly(ethylene) glycol molecules attached to surfaces in water is close to 3 nm.²⁷ Taking into consideration that the contact zone is not water only but instead a mixture of proteins, poly(ethylene)glycols and surfactants, the deduced value strongly supports our hypothesis of a solid self-organized assembly.

Conclusion

Emulsions as compared to vesicles probably allow some better control over the liquid interface composition and its surface energy. Here we have described adhesion experiments of droplets onto a solid substrate for which all parameters were measured and controlled. The careful analysis of our data suggests a scenario for specific wetting that involves also the role of non-specific contributions. Indeed, once proteins are grafted onto the liquid surface, their entropy is significantly reduced. This in turn facilitates the exploration of condensed states as a result of any weak non-specific interactions between the proteins and their surrounding medium within the confined layer. This effect is shown here to efficiently recruit mobile ligands. As a consequence, since in our case the substrate is solid, the specific binding takes place in the absence of translational diffusion. This causes a large decrease in the final density of specific bonds. However, this density still sets the final adhesive energy. We believe these experiments highlight the important role of weak non-specific attractive interactions in the formation and structuring of adhesive films.

Acknowledgements

We thank Dr Andrew Utada for the careful reading of the present manuscript.

References

- 1 G. I. Bell, M. Dembo and P. Bongrand, *Biophys. J.*, 1984, **45**, 1051–1064.
- 2 F. Pincet, E. Perez, J. C. Loudet and L. Lebeau, *Phys. Rev. Lett.*, 2001, **87**, 178101.
- 3 D. A. Nopp/Simson and D. Needham, *Biophys. J.*, 1996, **70**, 1391–1401.
- 4 J. Nam and M. M. Santore, *Langmuir*, 2007, **23**, 7216–7224.
- 5 B. M. Discher, Y. Y. Won, D. S. Ege, J. C. M. Lee, F. S. Bates, D. E. Discher and D. A. Hammer, *Science*, 1999, **284**, 1143–1146.
- 6 A. L. Bernard, M. A. Guedeau-Boudeville, O. Sandre, S. Palacin, J. M. di Meglio and L. Jullien, *Langmuir*, 2000, **16**, 6801–6808.
- 7 V. Marchi-Artzner, B. Lorz, C. Gosse, L. Jullien, R. Merkel, H. Kessler and E. Sackmann, *Langmuir*, 2003, **19**, 835–841.
- 8 R. Bruinsma, A. Behrisch and E. Sackmann, *Phys. Rev. E*, 2000, **61**, 4253–4267.
- 9 D. Iber, *Cell. Mol. Life Sci.*, 2005, **62**, 206–213.
- 10 G. T. Hermanson, *Bioconjugate Techniques*, Academic Press, New York, 1st edn, 1996.
- 11 N. M. Green, *Methods Enzymol.*, 1990, **184**, 51–67.
- 12 T. G. Mason and J. Bibette, *Phys. Rev. Lett.*, 1996, **77**, 3481–3484.
- 13 J. P. Helme, *Soybean Oil Refining – Technical Report*, American Soybean Oil Association – International Marketing Europe, Brussels, 1984.
- 14 H. M. Shapiro, *Practical Flow Cytometry*, John Wiley and Sons, New York, 4th edn, 2003.
- 15 J. Fattaccioli, J. Baudry, E. Bertrand, C. Goubault, N. Henry and J. Bibette, Size and fluorescence measurements of individual droplets by flow cytometry, submitted to Soft Matter, 2008.
- 16 S. Scheuring, D. J. Muller, P. Ringler, J. B. Heymann and A. Engel, *J. Microsc.*, 1999, **193**, 28–35.
- 17 A. Pierres, D. Touchard, A. M. Benoliel and P. Bongrand, *Biophys. J.*, 2002, **82**, 3214–3223.
- 18 D. Cuvelier and P. Nassoy, *Phys. Rev. Lett.*, 2004, **93**, 228101.
- 19 A. S. G. Curtis, *J. Cell Biol.*, 1964, **20**, 199–215.
- 20 S. R. Sheth and D. Leckband, *Proc. Natl. Acad. Sci. U. S. A.*, 1997, **94**, 8399–8404.
- 21 L. Cohen-Tannoudji, E. Bertrand, J. Baudry, C. Robic, C. Goubault, M. Pellissier, A. Johnner, F. Thalmann, N. K. Lee, C. M. Marques and J. Bibette, *Phys. Rev. Lett.*, 2008, **100**, 108301.
- 22 J. Drelich, *Colloids Surfaces A: Physicochem. Eng. Aspects*, 1996, **116**, 43–54.
- 23 S. Herminghaus and F. Brochard, *C. R. Phys.*, 2006, **7**, 1073–1081.
- 24 P. G. de Gennes, P. H. Puech and F. Brochard-Wyart, *Langmuir*, 2003, **19**, 7112–7119.
- 25 P. Ratanabankoon, M. Gropper, R. Merkel, E. Sackmann and A. P. Gast, *Langmuir*, 2003, **19**, 1054–1062.
- 26 N. K. Lee, A. Johnner, F. Thalmann, L. Cohen-Tannoudji, E. Bertrand, J. Baudry, J. Bibette and C. M. Marques, *Langmuir*, 2008, **24**, 1296–1307.
- 27 N. V. Efremova, B. Bondurant, D. F. O'Brien and D. E. Leckband, *Biochemistry*, 2000, **39**, 3441–3451.